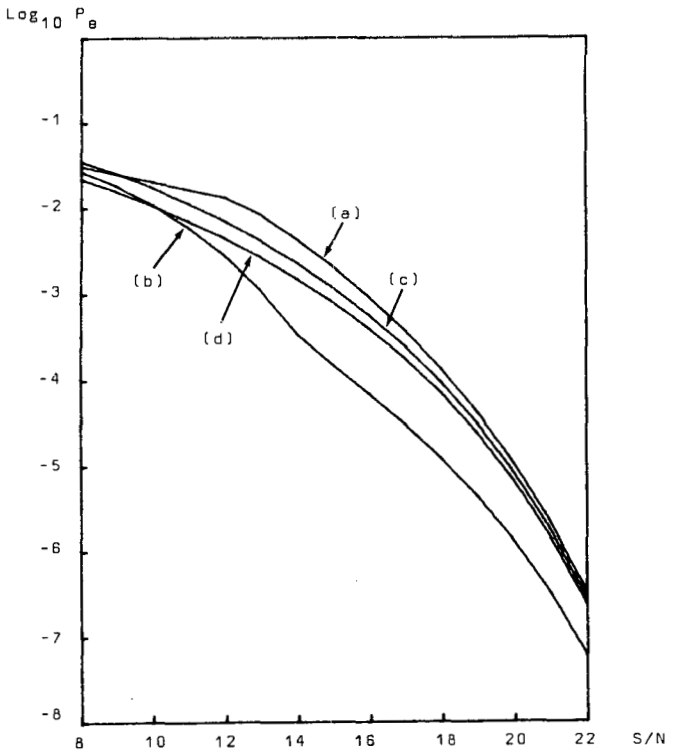

Figure 2. Bounds for the Raised Cosine Impulse Response (N = 30), with $0.2T$ Timing Error. (a) Best of the upper bounds used for comparison. (b) Best of the lower bounds used for comparison. (c) Proposed upper bound. (d) Proposed lower bound.

symbol interference and Gaussian noise. These formulas, which can be generalized to multilevel or multiphase signaling, compare favorably with previously published bounds of similar complexity, especially in the case of highly distorting channels and high S/N ratios.

The simplicity and tightness of the bounds make them a useful tool in these design situations when an approximation to the probability of error is required.

REFERENCES

[1] E. Y. Ho and Y. S. Yeh, "A New Approach for Evaluating the Error probability of Intersymbol Interference and Additive Gaussian Noise", *Bell Sys. Tech. J.* (Nov. 1970), pp. 2249-2265.

[2] F. S. Hill, Jr., "The computation of Error Probability for Digital Transmission", *Bell Sys. Tech. J.* (July-Aug. 1971), pp. 2055-2077.

[3] O. Shimbo and M. I. Celebiler, "The Probability of Error due to Intersymbol Interference and Gaussian Noise in Digital Communication Systems", *IEEE Trans. on Comm. Tech.*, (April 1971), pp. 113-119.

[4] Y. S. Yeh and E. Y. Ho, "Improved Intersymbol Interference Error Bounds in Digital Systems", *Bell Sys. Tech. J.* (Oct. 1971), pp. 2585-2598.

[5] V. K. Prabhu, "Some Considerations of Error Bounds in Digital Systems", *Bell Sys. Tech. J.* (Dec. 1971), pp. 3127-3151.

[6] B. R. Saltzberg, "Intersymbol Interference Error Bounds with Applications to Ideal Bandlimited Signalling", *IEEE Trans. on Inf. Th.* (July 1968), pp. 563-568.

[7] R. Lugannani, "Intersymbol Interference and Probability of Error in Digital Systems", *IEEE Trans. on Inf. Th.* (Nov. 1969), pp. 682-688.

[8] F. E. Glave, "An Upper Bound on the Probability of Error due to Intersymbol Interference for Correlated Digital Signals", *IEEE Trans. on Inf. Th.* (May 1972), pp. 356-363.

[9] J. W. Matthews, "Sharp Error Bounds for Intersymbol Interference", *IEEE Trans. on Inf. Th.* (July 1973), pp. 440-447.

[10] P. J. McLane, "Lower Bounds for Finite Intersymbol Interference Error Rates", *IEEE Trans. on Comm.* (June 1974), pp. 853-857.

[11] J. V. Murphy, "A Simple Approximation to Intersymbol Interference Error Rate for Low SNR", *IEEE Trans. on Inf. Th.* (Nov. 1975), pp. 682-687.

[12] K. Yao and R. M. Tobin, "Moment Space Upper and Lower Error Bounds for Digital Systems with Intersymbol Interference", *IEEE Trans. on Inf. Th.* (Jan. 1976), pp. 65-74.

[13] R. W. Lucky, J. Salz and E. J. Weldon, *Principles of Data Communications*, McGraw-Hill, 1968.

Improving QPSK Transmission in Band-Limited Channels with Interchannel Interference Through Equalization

S. H. R. RAGHAVAN AND R. E. ZIEMER

Abstract—**This paper describes the use of equalization in conjunction with channel filtering to improve QPSK transmission subject to both intersymbol interference (ISI) and interchannel interference (ICI). Performance bounds are computed using the nonclassical Gauss-quadrature rule (GQR) method. The signal-to-noise ratio (SNR) gain due to linear equalization over nonequalization is thereby obtained and presented.**

The performance of a linear equalizer thus obtained is compared with the Viterbi algorithm sequence estimator (VASE). In the absence of bounds for the VASE receiver under the channel conditions considered, simulation results are used to make the comparison. With a possible difference in the accuracies of the performance thus obtained it is shown that the VASE provides improved performance over the linear equalizer under the channel conditions considered.

I. INTRODUCTION

Equalization techniques have been considered by many authors [1]-[3] to minimize the adverse effects of intersymbol interference (ISI). Equalization is a technique by which adjustments are made in the received signal so as to increase the useful signal energy by decreasing the ISI. This can be achieved by using a tapped delay line, multipliers, and a summer. The received signal, delayed by the tapped delay line by various increments, is multiplied by tap weights, and the weighted increments added in a summer. Quite often the tap weights are adapted to the unknown channel response using an adjustment algorithm based on some criterion such as minimum-mean-square error (MMSE). In some cases feedback may be employed. It is not considered in this paper and hence the tapped-delay-line equalizer investigated is referred to as linear or a transversal filter.

Another important class of equalizers based on maximum-likelihood sequence estimation is the Viterbi algorithm sequence estimator. This structure in its earliest form consisted of a whitened matched filter and a Viterbi processor [4]. It

Paper approved by the Editor for Data Communication Systems of the IEEE Communications Society for publication after presentation at the National Telecommunications Conference, New Orleans, LA, December 1-3, 1975. Manuscript received April 7, 1976, revised May 9, 1977.

S. H. R. Raghavan with the School of Engineering Technology, University of Nebraska at Omaha, Omaha, NE 68101. He is now with the Collins Division of Rockwell International Group, Dallas, TX.

R. E. Ziemer is with the Department of Electrical Engineering, University of Missouri, Rolla, MO 65401.

has gone through several modifications [5], [6] in terms of simplicity in implementation.

In this paper a multichannel QPSK communication system in which the bandwidth of each channel is limited to minimize the adjacent channel interference is considered. Improvement gained through the use of channel filtering in conjunction with linear equalization is evaluated through performance bounds computed using the Gauss-quadrature rule (GQR) integration method [7]. Representative results to show the overall system performance improvement gained through the use of channel filtering and linear equalization are given. Also, the performance of the Viterbi algorithm sequence estimator (VASE) obtained through simulation is compared with that of a linear equalizer. The results clearly indicate that the VASE receiver can give superior performance to that of a linear equalizer under the channel conditions considered.

II. SYSTEM DESCRIPTION

A block diagram for the communication system is shown in Fig. 1. The complex envelope of the transmitted signal is [8],

$$\tilde{S}_{\mathrm{tr}}(t) = \sum_{n=-\infty}^{\infty} e^{j\theta_n(t)} \tag{1}$$

where $\theta_n(t) = \pm\pi/4, \pm 3\pi/4$; $nT \leqslant t \leqslant (n+1)T$. Similarly, the complex envelope of the signal from the lth interfering channel is

$$\tilde{S}_{\mathrm{tr}}(t) = \sum_{n_l=-\infty}^{\infty} e^{j[\theta_{n_l}(t-\epsilon_l T)+\psi_l]} \tag{2}$$

where θ_n is the phase of nth symbol in the lth channel, ϵ_l is the normalized misalignment of the symbol n_l and ψ_l is the carrier phase incoherence.

The complex envelope of the filter impulse response at the output of the lth modulator can be written as

$$h_l(t) = h_0(t)e^{jl\omega_d t} \tag{3}$$

where $h_0(t)$ is the impulse response of a symmetrically band-limited equivalent low-pass filter at the transmitter in the useful channel and ω_d is the frequency spacing between two adjacent channels. Now, if the number of interfering channels below the carrier frequency ω_0 is N_b, and the number above is N_a, the complex envelope of the signal at the receiver filter input can be written as

$$\tilde{S}_{\mathrm{ch}}(t) = \sum_{l=-N_b}^{N_a} \beta_l(t) \sum_{n_l=-\infty}^{\infty} e^{j[\theta_{n_l}(t-\epsilon_l T)+l\omega_d t+\psi_l]} * h_l(t) \tag{4}$$

where $\beta_l(t)$ is the attenuation factor of the lth channel signal and $*$ denotes convolution.

A block diagram of the receiver with linear equalizer is given in Fig. 2. The receiver filter serves the dual purpose of reducing the out-of-band noise as well as the interchannel interference (ICI). The second operation performed by the receiver is synchronous demodulation with reference signals which are in phase quadrature. The demodulated signal is equalized using a transversal filter. When the channel response is not known,

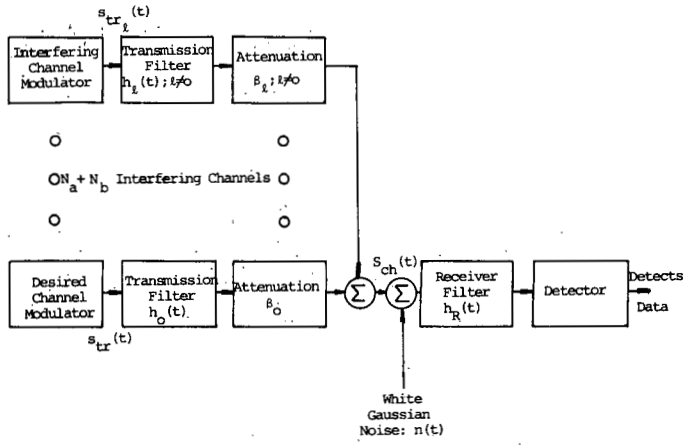

Fig. 1. Communication system block diagram.

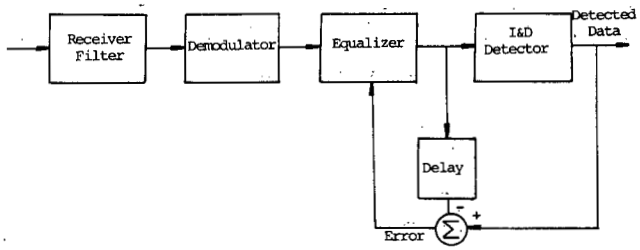

Fig. 2. Block diagram of the receiver with adaptive linear equalizer.

or if the channel response is slowly time varying, the complex tap weights, $\tilde{W}_{rj} = W_{rrj} + jW_{rij}$ and $\tilde{W}_{ij} = W_{iij} + jW_{irj}$, are determined adaptively to minimize the mean-square error at the equalizer output. If W_{rrj}, W_{rij}, W_{irj}, and W_{iij} are the equalizer tap weights, as shown in Fig. 3, the estimate-gradient algorithms to adjust the equalizer tap weights are given by [6]

$$W_{rrj}(n+1) = W_{rrj}(n) - \alpha\left[\sum_{k=1}^{N_s} (W_{rrk}z_r + W_{irk}z_i - d_1)z_r\right], \tag{5}$$

$$W_{iij}(n+1) = W_{iij}(n) - \alpha\left[\sum_{k=1}^{N_s} (W_{iik}z_i - W_{rik}z_r - d_2)z_i,\right] \tag{6}$$

$$W_{rij}(n+1) = W_{rij}(n) + \alpha\left[\sum_{k=1}^{N_s} (W_{iik}z_i - W_{rik}z_r - d_2)z_r\right], \tag{7}$$

and

$$W_{irj}(n+1) = W_{irj}(n) - \alpha\left[\sum_{k=1}^{N_s} (W_{rrk}z_r + W_{irk}z_i - d_1)z_i\right], \tag{8}$$

where α is a constant which determines the rate of tap-weight convergence and influences the amount of tap-adjustment noise generated during equalizer adaptation, d_1 and d_2 are the detected data at the in-phase and quadrature channel outputs obtained by integrate-and-dump detecting the equalizer output, z_r and z_i are the demodulator outputs in the in-phase

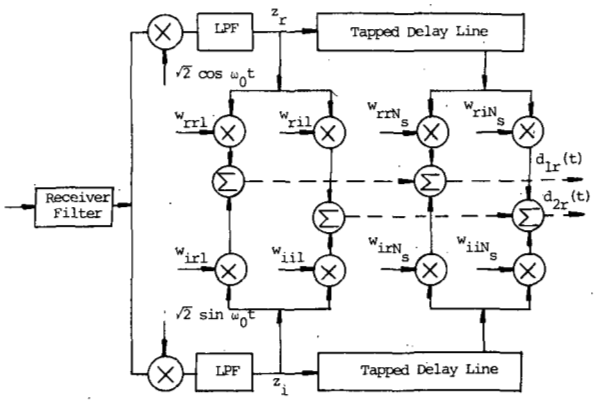

Fig. 3. QPSK equalizer at *RF*.

and the quadrature channels, and N_s is the number of equalizer stages.

A block diagram of the receiver with an adaptive VASE [4] is given in Fig. 4. The VASE considered here is based on the structure proposed by Falconer and Magee [9]. The receiver consists of a linear prefilter, the Viterbi processor, and a desired impulse response filter (DIRF). The linear prefilter is adjusted in such a way that the impulse response of the channel prefilter combination is approximately equal to the DIRF which is chosen to be of short duration. This DIRF impulse response is used in the Viterbi processor for the maximum-likelihood sequence estimation of the received data. Again, the linear prefilter tap weights $\tilde{W}_j = W_{rj} + jW_{ij}$, and DIRF tap weights, $\tilde{v}_j = v_{rj} + jv_{ij}$, are determined to minimize the mean-square error at the equalizer output and the energy in the DIRF tap weights is constrained to be unity. If W_{rj} and W_{ij} are the prefilter tap weights and v_r and v_i are the DIRF tap weights as shown in Fig. 5, the estimate-gradient algorithms to adjust these weights are given by [9]

$$W_{rj}(n+1) = W_{rj}(n) - \alpha_1 [e_r(n)z_r(n - N_D - j + 1) + e_i(n)z_i(n - N_D - j + 1)] \quad (9)$$

$$W_{ij}(n+1) = W_{ij}(n) - \alpha_1 [e_r(n)z_i(n - N_D - j + 1) - e_i(n)z_r(n - N_D - j + 1)] \quad (10)$$

where

$$e_r(n) = \text{Re}\,[\tilde{e}(n)]$$

$$e_i(n) = \text{Im}\,[\tilde{e}(n)]$$

$$\tilde{e}(n) = \tilde{d}(n - N_D) - \tilde{f}(n - N_D).$$

Here $\tilde{d}(n - N_D)$ is the linear prefilter output and $\tilde{f}(n - N_D)$ is the DIRF output. Similarly, we obtain the estimate-gradient algorithms to adjust v_i and v_r as

$$v_{r'j}(n+1) = v_{rj}(n) + \alpha_2 [e_r(n)I_r(n - N_D - j + 1) + e_i(n)I_i(n - N_D - j + 1)] \quad (11)$$

$$v_{i'j}(n+1) = v_{ij}(n) + \alpha_2 [e_r(n)I_i(n - N_D - j + 1) - e_i(n)I_r(n - N_D - j + 1)] \quad (12)$$

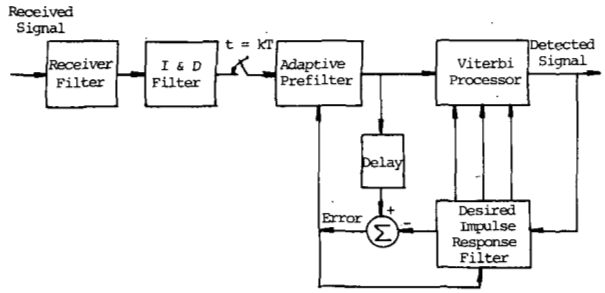

Fig. 4. Block diagram of the adaptive VASE.

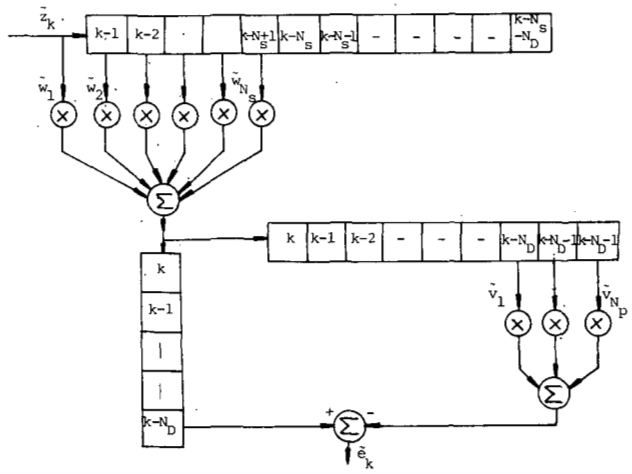

Fig. 5. Maximum-likelihood sequence estimator in complex envelope representation.

where $I_r(\cdot)$ and $I_i(\cdot)$ are the detected bits in the in-phase and the quadrature channels, which are normalized as

$$v_{rj}(n+1) = \frac{v_{r'j}(n+1)}{[|v_{r\,j}(n+1)|^2 + |v_{i\,j}(n-1)|^2]} \quad (13)$$

$$v_{ij}(n+1) = \frac{v_{i,j}(n+1)}{[|v_{r'j}(n+1)|^2 + |v_{i'j}(n+1)|^2]}. \quad (14)$$

Here again, α_1 and α_2 are the tap-adjustment parameters which perform the same function as α in (5)–(8).

III. COMPUTER SIMULATION

The computer evaluation of the linear equalizer was done in two steps by employing separate computer programs. In the first step, a simulation model developed in the study of multipath effects on QPSK transmission [3] was modified to include ICI effects. In the second step, bounds for the probability of error for the linear equalizer operating in ISI and ICI were computed using the GQR integration method. The results from these two steps were used to complement and verify each other.

In the simulation, the data sequence for the useful channel is simulated by a 31-bit maximal-length pseudonoise sequence and the data sequences in the interfering adjacent channels are simulated by 63-bit and 127-bit maximal-length pseudonoise sequences. The simulation is done over six sequence periods. During the first two sequence periods, equalizer tap

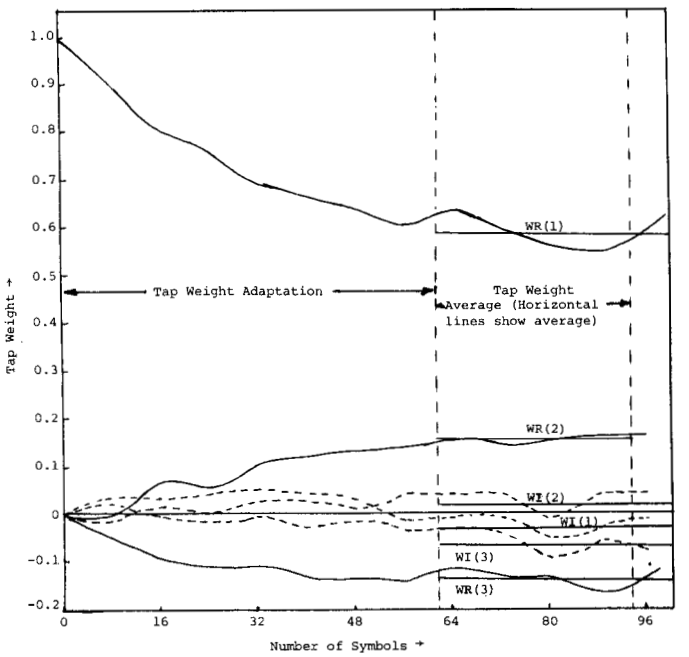

Fig. 6. Tap weights versus number of symbols for linear adaptive equalizer.

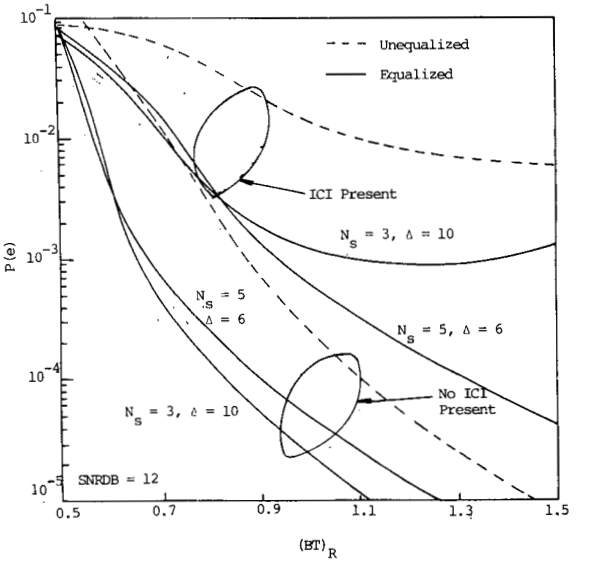

Fig. 7. Performance as a function of time-bandwidth product BT of receiver filter for $N_{eq} = 1; 3$ and 5 taps; $N_s\Delta = 30$.

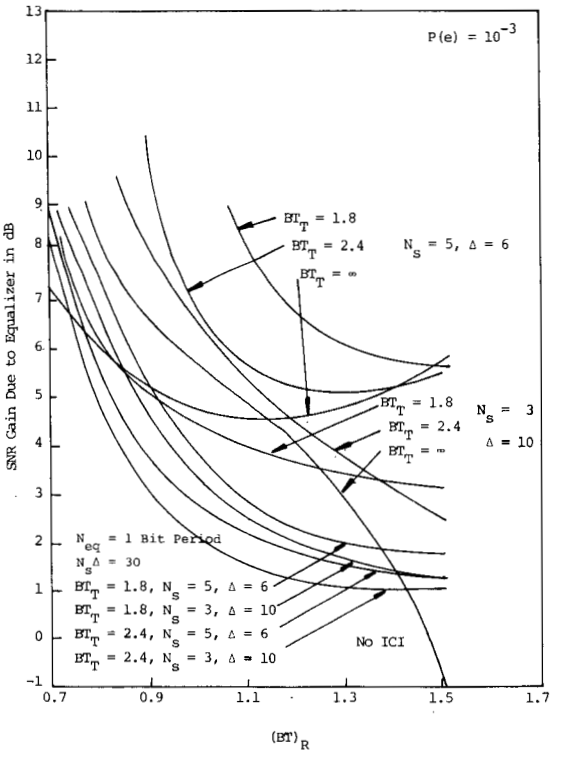

Fig. 8. SNR gain due to equalizer as a function of time-bandwidth product $(BT)_R$; $N_{eq} = 1$; $N_s\Delta = 30$.

weights are adjusted adaptively. In the next sequence period the tap weights are averaged to minimize the effect of tap-adjustment noise, and the tap weights are frozen at these average values. A typical tap-adaptation sequence is shown in Fig. 6 along with the final average tap weights. In the last three sequence periods, the probability of symbol error is computed for each symbol using the fact that the equalizer is linear and the sequences are deterministic. The symbol-error probabilities are then averaged over the three sequence periods to give the average probability of symbol error.

In the second step of the linear equalizer evaluation, the steady-state averaged values of the tap weights are used in the computation of the bounds by the GQR method [7]. For simplicity, the equalizer output is sampled at the end of each bit period instead of at a time when the impulse response of the overall system is maximum. To keep the computation time small, only three terms in the Gauss-quadrature summation and three interfering symbols are considered.

Probability of symbol-error results from step one of the evaluation were used to verify the accuracy of the bounds thus computed.

The Monte Carlo simulation of the VASE receiver consists of generating sequences in the useful channel and in the interfering adjacent channels using 31-bit, 63-bit, and 127-bit pseudonoise sequences. Gaussian noise of mean zero and appropriate variance is added separately to the in-phase and quadrature channel signals. The simulation is done over 5000 symbols (some results were checked with 10 000 data symbols) after the tap weights have settled to their steady-state values. Comparison of the detected symbol with the delayed version of the transmitted symbol results in the number of errors made in detection and the relative frequency of error is then computed. For 10 000 transmissions, one can therefore expect a reasonably accurate determination of values of P_e in the neighborhood of 0.001.

IV. RESULTS

Representative results obtained through bound computation and computer simulation are shown in Figs. 7–10. In these figures, N_{eq} refers to the number of bit periods over which equalization is performed, N_s is the number of equalizer stages and Δ is the equalizer tap spacing. In all the results presented here, second-order Butterworth filters are used, both at the transmitter and the receiver. Also, the impulse response of the DIRF in the VASE receiver is restricted to 3-bit periods.

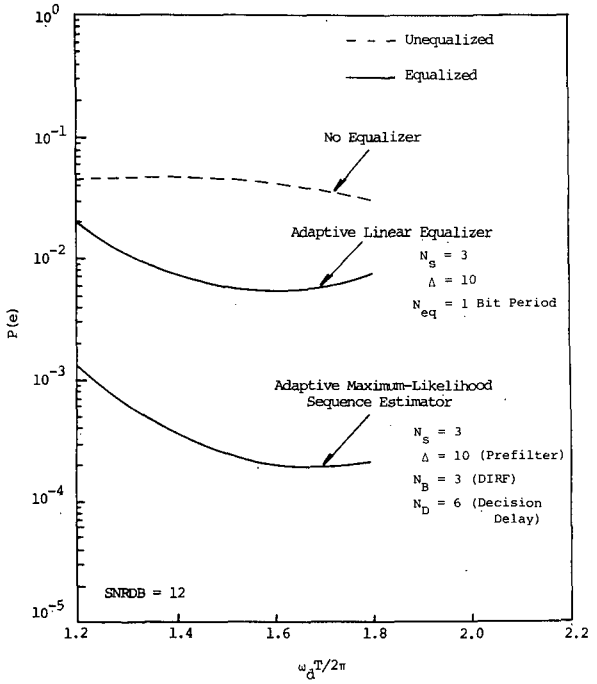

Fig. 9. Performance comparison of adaptive linear equalizer and VASE as a function of frequency offset of ICI.

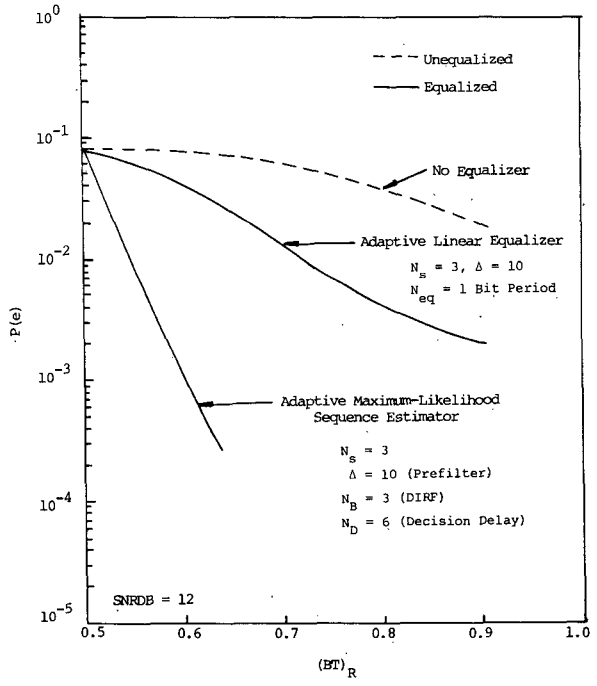

Fig. 10. Performance comparison of adaptive linear equalizer and VASE as a function of $(BT)_R$.

In Fig. 7, the probability of symbol-error versus time-bandwidth product, $(BT)_R$ (T is the bit period), of the receiver filter is given. At smaller values of $(BT)_R$ ISI is dominant in degrading the performance, and at larger $(BT)_R$ values ICI is dominant in degrading receiver performance. Note that the equalizer provides a significant improvement even at large $(BT)_R$ values where the degradation due to ICI is dominant. In Fig. 8, SNR gain, defined to be the increase in SNR necessary to maintain a specified probability of error, P_e, in this case 10^{-3}, when the received signal is unequalized is shown. As shown in this figure and in most of the cases considered, SNR gain when both ISI and ICI are present is higher than when only ISI is present, indicating the improvement gained due to the equalizer when the received signal is subject to both ISI and ICI.

The performance of the receiver with an adaptive linear equalizer is compared with that of a receiver with the VASE in Figs. 9 and 10. In Fig. 9 the probability of symbol error is plotted versus normalized frequency offset for both the linear equalizer and VASE as well as a receiver with no equalizer. In Fig. 10 similar results with receiver filter time-bandwidth product as the abscissa are given. From both of these figures we see that the VASE has superior performance to that of an adaptive linear equalizer under the conditions simulated.

It should be noted that two different methods were used to obtain the performance of the linear equalizer and the VASE receiver as explained in the previous section. Since the performance bound calculation used to evaluate the linear equalizer is more accurate than the Monte Carlo simulation used to evaluate the VASE receiver, the actual improvement of the VASE over the linear equalizer may differ from that shown in Figs. 9 and 10.

The noise and the channel conditions were maintained the same for both linear equalizer and VASE receiver in order to get as fair a comparison as possible. In the case of the VASE receiver at large interference levels, the prefilter and DIRF coefficients were more sensitive to the tap-adjustment coefficients α_1 and α_2.

REFERENCES

[1] R. W. Lucky, "Automatic equalization for digital communication," *Bell Syst. Tech. J.*, vol. 44, pp. 547–588, Apr. 1965.

[2] P. Monsen, "Feedback equalization for fading dispersive channels," *IEEE Trans. Inform. Theory*, vol. IT-17, pp. 56–64, Jan. 1971.

[3] C. R. Ryan and R. E. Ziemer, "Adaptive equalizer for high data rate QPSK transmission in two-component multipath," in *Conf. Rec., Int. Conf. Communications*, June 1973, pp. 18-4–18-8.

[4] G. D. Forney, Jr., "Maximum-likelihood sequence estimation of digital sequences in the presence of intersymbol interference," *IEEE Trans. Inform. Theory*, vol. IT-18, pp. 363–378, May 1972.

[5] F. R. Magee, Jr., "Adaptive maximum-likelihood sequence estimation for digital signaling in the presence of intersymbol interference," *IEEE Trans. Inform. Theory*, vol. IT-19, pp. 699–702, Sept. 1973.

[6] S. H. R. Raghaven, "Use of adaptive linear equalization and maximum-likelihood sequence estimation in conjunction with filtering to improve QPSK communication in intersymbol and interchannel interference channels," Ph. D. dissertation, University of Missouri-Rolla, Aug. 1975.

[7] S. Benedetto, E. Biglieri, and V. Castellani, "Combined effects of intersymbol, interchannel, and cochannel interferences in M-ary CPSK systems," *IEEE Trans. Commun.*, vol. COM-21, pp. 997–1008, Sept. 1973.

[8] S. H. R. Raghaven and R. E. Ziemer, "Comparison of linear equalization and Viterbi algorithm estimation for improving QPSK transmission in bandlimited channels with interchannel interferences," in *Nat. Telecommunications Conf. Proc.*, vol. 2, Dec. 1975, pp. 39-24–39-28.

[9] D. D. Falconer and F. R. Magee, Jr., "Adaptive channel memory truncation for maximum-likelihood sequence estimation," *Bell Syst. Tech. J.*, pp. 1541–1562, Nov. 1973.

[10] G. D. Forney, Jr., "The Viterbi algorithm," *IEEE Proc.*, vol. 61, pp. 268–278, Mar. 1973.